DISCRETE AND CONTINUOUS
DYNAMICAL SYSTEMS SERIES S
Volume **14**, Number **7**, July **2021**

doi:10.3934/dcdss.2020176

pp. **2261–2272**

A NOVEL MODEL FOR THE CONTAMINATION OF A SYSTEM OF THREE ARTIFICIAL LAKES

Veysel Fuat Hatipoğlu

Muğla Sıtkı Koçman University
Muğla, 48300, Turkey

Abstract. In this study, a new model has been developed to monitor the contamination in connected three lakes. The model has been motivated by two biological models, i.e. cell compartment model and lake pollution model. Haar wavelet collocation method has been proposed for the numerical solutions of the model containing a system of three linear differential equations. In addition to the solutions of the system, convergence analysis has been briefly given for the proposed method. The contamination in each lake has been investigated by considering three different pollutant input cases, namely impulse imposed pollutant source, exponentially decaying imposed pollutant source, and periodic imposed pollutant source. Each case has been illustrated with a numerical example and results are compared with the exact ones. Regarding the results in each case it has been seen that, Haar wavelet collocation method is an efficient algorithm to monitor the contamination of a system of lakes problem.

1. **Introduction.** Pollution of water resources such as rivers, lakes, etc. is one of the major issues of environmental pollution. Here we employ with the pollution in the artificial lakes system. In order to monitor the pollution in lakes setting up a mathematical model and then finding the pollution level in connected three lakes is much cheaper than experimenting this phenomena in the real world. For this purpose we consider a system of three artificial interconnecting lakes with various pollution input sources. We are inspired by two well-known mathematical models in biology to figure out the model. The first one is a compartment model, important especially in screening the drugs used by humans. Compartment models are widely used for describing the drug propagation in the human body. A system of two compartments is

$$\begin{cases} \frac{\mathrm{d}u_1(t)}{\mathrm{d}t} = k\left(\frac{u_2}{V_2} - \frac{u_1}{V_1}\right), \\ \frac{\mathrm{d}u_2(t)}{\mathrm{d}t} = k\left(\frac{u_1}{V_1} - \frac{u_2}{V_2}\right), \end{cases} \tag{1}$$

where k is proportionality constant, u_i denotes the mass of molecule and V_i denotes the volume of the compartment i. We refer the interested reader to recent papers [10] and [20] for recent applications of compartment models. We are also inspired by another mathematical model in biology, a lake pollution model [1],

$$\frac{\mathrm{d}m(t)}{\mathrm{d}t} = c_{in}(t)F_{in}(t) - c_{out}(t)F_{out}(t), \tag{2}$$

2020 *Mathematics Subject Classification.* Primary: 34A30, 65L05; Secondary: 92-08.

Key words and phrases. Haar wavelets, collocation methods, lake contamination problem, compartment model.

where m is the mass of the pollutant, c is concentration of the pollutant, F denotes the flow rate, *in* and *out* represents the direction of flow. In order to model the

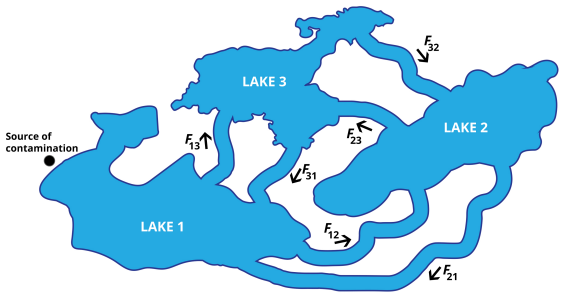

FIGURE 1. Illustration of the interconnected Lakes 1, 2, 3, and flow F_{12}, F_{13}, F_{21}, F_{23}, F_{31}, F_{32}.

considered system we assume the volume of the each lake, the flow rate and the reaction rate remain constant. Moreover we consider each lake as well mixed. The main idea of developing our model is supposing each lake like a compartment as in (1). So the flow between the lakes behaves like the molecules traveling between the compartments in the process. Within this frame, model of the contamination problem of interconnecting three lakes with channels could be developed by mixing the (1) and (2) as the following system.

$$\begin{cases} \frac{\mathrm{d}u_1(t)}{\mathrm{d}t} = \frac{F_{21}}{V_2}u_2(t) + \frac{F_{31}}{V_3}u_3(t) + f(t) - \frac{F_{12}}{V_1}u_1(t) - \frac{F_{13}}{V_1}u_1(t), \\ \frac{\mathrm{d}u_2(t)}{\mathrm{d}t} = \frac{F_{12}}{V_1}u_1(t) + \frac{F_{32}}{V_3}u_3(t) - \frac{F_{21}}{V_2}u_2(t) - \frac{F_{23}}{V_2}u_2(t), \\ \frac{\mathrm{d}u_3(t)}{\mathrm{d}t} = \frac{F_{13}}{V_1}u_1(t) + \frac{F_{23}}{V_2}u_2(t) - \frac{F_{32}}{V_3}u_3(t) - \frac{F_{31}}{V_3}u_3(t) \end{cases} \tag{3}$$

with the initial conditions

$$u_1(0) = \lambda_1, \quad u_2(0) = \lambda_2, \quad u_3(0) = \lambda_3.$$

Here, $u_1(t), u_2(t)$, and $u_3(t)$ are the amount of pollutant in each lake at time t, the function $f(t)$ denotes the rate of pollutant entering the Lake 1 per unit time t. F_{ij} denotes the water flow from lake i to lake j and V_i denotes the volume of lake i. In order to ensure the constant volume in each lake we assume

$$\begin{aligned} F_{12} &= F_{21} + F_{31} - F_{13}, \\ F_{23} &= F_{12} + F_{32} - F_{21}. \end{aligned} \tag{4}$$

The visualization of the lake contamination model is presented in Figure 1 for the sake of convenience of the reader.

In the literature (See [11]), it is seen that Haar wavelet collocation method has efficient results for the approximate solutions for the system of linear ordinary differential equations. Therefore here we focused on Haar wavelet collocation method to obtain the solution of the system (3). Haar wavelet techniques have been attracting several scientists in the field of numerical computation. In 2005, Lepik offers solutions for both ordinary differential equations and partial differential equations by using Haar wavelet techniques [11]. A Haar wavelets based efficient method was proposed by Çelik in [4] for the solutions of nonlinear partial differential equations and applied to generalized Burgers-Huxley equation. In [8], a Haar wavelets based

approach was performed for solution of a prototypical reaction-diffusion equation, Fisher's equation. The study presented in [16], solves fractional-order differential equations of the linear multi-point boundary value problems by employing a numerical algorithm which is based on Haar wavelet operational matrices of integration. Rehman and Khan have obtained the solutions of boundary value problems for linear fractional partial differential equations by using Haar wavelets in [17]. Within the frame of gene propagation and biological modeling the Burger's equation, Cahn-Allen equation, Fisher's equation, Fitz-Hugh-Nagumo equation, and the Nowell-Whitehead equation were solved by using Haar wavelet or Haar transform method in [6]. Approximate solution of convection-diffusion equations by using Haar wavelet method has obtained by Singh and Kumar in [19]. In [14], the fractional-order integration is derived by Haar wavelet operational matrix and it is used in order to solve composite fractional oscillation equations and also some of the fractional-order differential equations such as the Ricatti and Bagley-Torvik equations. A Haar wavelets based numerical approach was presented in [12] to solve the nonlinear integral equations. It is seen that, the proposed method can be used for solving ordinary differential equations with boundary values and it is applicable for Volterra integral and integro-differential equations. In recent paper [15], Haar wavelet method has been applied to one dimensional coupled KdV equation to find their numerical solutions. In [13], the author performs solutions for nonlinear evolution equations by using an efficient numerical method based on the Haar wavelets. The proposed method was applied to the Burger's and sine-Gordon equations. By applying Haar wavelets, the authors in [21] presented approximate solutions for Bratu-type equations which arise in fuel oxidization of the heat transfer applications and combustion theory. A Haar wavelet based method implementation was presented in [7] in order to describe the reckoning of soil temperature at different depths. Reduction of the the fractional Abel and Volterra integral equations into an algebraic equations system was performed in paper of [18] by using a Haar wavelet approximating method. In [2], an approximate solution of Fredholm and Volterra integro-differential equations of second kind was presented by using a new Haar wavelets approximation based method.

Some different lake pollution models have been solved by various numerical approaches. For instance, a collocation method based on Bessel polynomials is applied in [22], and differential transform method is applied in [3]. Motivated by previous studies, our aim is to apply Haar wavelet collocation method in order to obtain an approximate solution for the model (3). For this purpose, the system (3) by Haar functions is expressed in the form

$$u_j(t) \quad = \quad \sum_{i=0}^{m-1} a_{i,j} h_i(t), \quad j = 1, 2, 3 \tag{5}$$

where $a_{i,j}, i = 0, 1, ..., m-1$ are the unknown Haar coefficients, $h_i(t), i = 0, 1, ..., m-1$ are the Haar functions that are defined in the next section.

2. Haar wavelets and function approximation.

In this section, basic notations and definitions on Haar wavelets are summarized. Then approximation by Haar function is given. Haar wavelet family for $t \in [0, 1)$ is defined by

$$h_i(t) = \begin{cases} 1 & , \quad for \quad t \in [\alpha, \beta) \\ -1 & , \quad for \quad t \in [\beta, \gamma) \\ 0 & , \quad otherwise \end{cases} \tag{6}$$

where

$$\alpha = \frac{k}{m}, \quad \beta = \frac{k+0.5}{m}, \quad \gamma = \frac{k+1}{m}.$$

The level of the wavelet is indicated by the $m = 2^j$ where $j = 0, 1, ..., J$ for the maximal level of resolution J. Also note that $k = 1, 2, ..., m-1$ is the translation parameter and i is calculated by the formula $i = m + k + 1$. The minimal value of i is $i = 2$ for $m = 1$ and $k = 0$, and the maximal value is $i = 2M = 2^{J+1}$. $h_1 \equiv 1$ in $[0, 1)$ is assumed to be the scaling function for $i = 1$. The integral of equation (6) is as follows:

$$p_{i,1}(t) = \int_0^t h_i(x)dx \tag{7}$$

and by integrating (7), we get

$$p_{i,1}(t) = \begin{cases} t-\alpha & , \quad for \quad t \in [\alpha, \beta) \\ \gamma - t & , \quad for \quad t \in [\beta, \gamma) \\ 0 & , \quad otherwise. \end{cases} \tag{8}$$

Let the collocation points be $t_l = (l - 0.5)/2M$, for $l = 1, 2, ..., 2M$ and the discretized Haar function $h_i(t)$. By this way we obtain the $2M \times 2M$ dimensional matrix of coefficients $H(i, l) = (h_i(t_l))$. The $2M \times 2M$ dimensional operational matrix $\mathbf{P}$ for integration is defined by

$$(PH)_{il} \quad = \quad \int_0^{t_l} h_i(t)dt. \tag{9}$$

The entries of matrices $\mathbf{P}$ and $\mathbf{H}$ are evaluated in [5] by using (8) and (9).

$$H_2 = \begin{pmatrix} 1 & 1 \\ 1 & -1 \end{pmatrix}, \; H_4 = \begin{pmatrix} 1 & 1 & 1 & 1 \\ 1 & 1 & -1 & -1 \\ 1 & -1 & 0 & 0 \\ 0 & 0 & 1 & -1 \end{pmatrix},$$

$$P_2 = \frac{1}{4}\begin{pmatrix} 2 & -1 \\ 1 & 0 \end{pmatrix}, \; P_4 = \frac{1}{16}\begin{pmatrix} 8 & -4 & -2 & -2 \\ 4 & 0 & -2 & 2 \\ 1 & 1 & 0 & 0 \\ 1 & -1 & 0 & 0 \end{pmatrix}.$$

In [5] the authors stated that the following matrix equation holds for calculating the matrix $\mathbf{P}$ of order $m = 2^j$, where j is positive integer.

$$P_{(m)} = \frac{1}{2m}\begin{pmatrix} 2mP_{(m/2)} & -H_{(m/2)} \\ H^{-1}_{(m/2)} & O \end{pmatrix},$$

where O is a null matrix of order $\frac{m}{2} \times \frac{m}{2}$. Here H_m is

$$H_{(m)} = \begin{bmatrix} h_0(t) \\ h_1(t) \\ \vdots \\ h_{m-1}(t) \end{bmatrix},$$

where Haar functions $h_i(t)$ for $i = 0, 1, ..., m-1$ are in row vector form. After calculating for $P_{(m)}$ and $H_{(m)}$, both matrices will be applicable for solving any differential equations.

The convergence analysis of Haar wavelet series is investigated in [9]. The following theorem is stated and proved in order to show the convergence rate analysis of Haar wavelets.

Theorem 2.1. *Assume that $u(t) \in L^2(\mathbb{R})$ with the bounded first derivative on $(0,1)$, then the following inequality holds.*

$$\|e_J(x)\| \leq \sqrt{\frac{L}{7}} K 2^{(-3)2^{J-1}}, \tag{10}$$

where K, L are some real constants and J is a positive number denoting maximal level of resolution of the wavelet.

From (10), one can see that the error bound is inversely proportional J. Therefore the convergence of the Haar wavelet approximation is guaranteed when J is increased. Next, we present the function approximation by using Haar function. Any function $u(t) \in L^2[0,1)$ can be decomposed as

$$u(t) = \sum_{i=0}^{\infty} c_i h_i(t), \tag{11}$$

where the coefficients c_i are determined by

$$c_i = 2^j \int_0^1 u(t) h_i(t) \mathrm{d}t, \tag{12}$$

where $i = 2^j + k$, $0 \leq k < 2^j$ and $j \geq 0$. Particularly $c_0 = \int_0^1 u(t)\mathrm{d}t$. The series expansion of $u(t)$ has an infinite terms. As long as $u(t)$ is a piecewise constant function, or approximated as a piecewise constant function for each subinterval, $u(t)$ will be concluded at finite terms as,

$$u(t) = \sum_{i=0}^{m-1} c_i h_i(t) = c_{(m)}^{\mathrm{T}} h_{(m)}(t), \tag{13}$$

where $c_{(m)}^{\mathrm{T}}$, $h_{(m)}(t)$, and $p_{(m)}(t)$ are defined as

$$c_{(m)}^{\mathrm{T}} = [c_0, c_1, ..., c_{m-1}],$$

$$h_{(m)}(t) = [h_0(t), h_1(t), ..., h_{m-1}(t)]^{\mathrm{T}},$$

and

$$p_{(m)}(t) = [p_{0,1}(t), p_{1,1}(t), ..., p_{m-1,1}(t)]^{\mathrm{T}},$$

where T denotes transpose and $m = 2^j$.

3. **Numerical solution.** In this section numerical solution of the system (3) is obtained. First, modifying (6) and (7) according to (3), we have

$$u_j'(t) = \sum_{i=0}^{m-1} a_{i,j} h_i(t) = a_{m,j}^{\mathrm{T}} h_{(m)}(t), \quad j = 1,2,3 \tag{14}$$

$$u_j(t) = \sum_{i=0}^{m-1} a_{i,j} p_{i,1}(t) = a_{m,j}^{\mathrm{T}} p_{(m)}(t) + u_j(0), \quad j = 1,2,3. \tag{15}$$

Then, imposing (14) and (15) into (3), we have that

$$\begin{cases} a_{(m,1)}^{\mathrm{T}} h_{(m)}(t) = & a_{(m,2)}^{\mathrm{T}} p_{(m)}(t) + u_2(0) + a_{(m,3)}^{\mathrm{T}} p_{(m)}(t) \\ & +u_3(0) + f(t) - a_{(m,1)}^{\mathrm{T}} p_{(m)}(t) - u_1(0), \\ a_{(m,2)}^{\mathrm{T}} h_{(m)}(t) = & a_{(m,1)}^{\mathrm{T}} p_{(m)}(t) + u_1(0) + a_{(m,3)}^{\mathrm{T}} p_{(m)}(t) \\ & -u_3(0) - a_{(m,2)}^{\mathrm{T}} p_{(m)}(t) - u_2(0), \\ a_{(m,3)}^{\mathrm{T}} h_{(m)}(t) = & a_{(m,1)}^{\mathrm{T}} p_{(m)}(t) + u_1(0) + a_{(m,2)}^{\mathrm{T}} p_{(m)}(t) \\ & +u_2(0) - a_{(m,3)}^{\mathrm{T}} p_{(m)}(t) - u_3(0). \end{cases}$$

By using the collocation points $t = t_l$ and the initial conditions $u_j(0) = 0$ for $j = 1, 2, 3$, we obtain

$$\begin{cases} a_{(m,1)}^{\mathrm{T}}(H_{(m)} + P_{(m)}H_{(m)}) - a_{(m,2)}^{\mathrm{T}} P_{(m)}H_{(m)} - a_{(m,2)}^{\mathrm{T}} P_{(m)}H_{(m)} = f(t_l), \\ -a_{(m,1)}^{\mathrm{T}} P_{(m)}H_{(m)} + a_{(m,2)}^{\mathrm{T}}(H_{(m)} + P_{(m)}H_{(m)}) - a_{(m,3)}^{\mathrm{T}} P_{(m)}H_{(m)} = 0, \\ -a_{(m,1)}^{\mathrm{T}} P_{(m)}H_{(m)} - a_{(m,2)}^{\mathrm{T}} P_{(m)}H_{(m)} + a_{(m,3)}^{\mathrm{T}}(H_{(m)} + P_{(m)}H_{(m)}) = 0. \end{cases}$$

Denoting the above system in the matrix-vector form, we have

$$\mathbf{Ac} = \mathbf{B}, \tag{16}$$

where

$$\mathbf{A} = \begin{pmatrix} A_{11} & A_{12} & A_{13} \\ A_{21} & A_{22} & A_{23} \\ A_{31} & A_{32} & A_{33} \end{pmatrix}, \quad \mathbf{B} = \begin{pmatrix} B_1 \\ B_2 \\ B_3 \end{pmatrix}, \quad \mathbf{c} = \begin{pmatrix} a_{(m,1)} \\ a_{(m,2)} \\ a_{(m,3)} \end{pmatrix}.$$

Here the dimensions of the matrices $\mathbf{A_{ij}}, (i = 1, 2, 3; j = 1, 2, 3)$ are $m \times m$, the dimensions of the matrices B_1, B_2 and B_3 are $m \times 1$. Therefore, the dimensions of the matrices $\mathbf{A}$, $\mathbf{B}$ and $\mathbf{c}$ are $3m \times 3m$, $3m \times 1$ and $3m \times 1$, respectively. Besides,

$$\begin{array}{lll} A_{11} = (H_{(m)} + P_{(m)}H_{(m)})^{\mathrm{T}}, & A_{12} = -(P_{(m)}H_{(m)})^{\mathrm{T}}, & A_{13} = -(P_{(m)}H_{(m)})^{\mathrm{T}}, \\ A_{21} = -(P_{(m)}H_{(m)})^{\mathrm{T}}, & A_{22} = (H_{(m)} + P_{(m)}H_{(m)})^{\mathrm{T}}, & A_{23} = -(P_{(m)}H_{(m)})^{\mathrm{T}}, \\ A_{31} = -(P_{(m)}H_{(m)})^{\mathrm{T}}, & A_{32} = -(P_{(m)}H_{(m)})^{\mathrm{T}}, & A_{33} = (H_{(m)} + P_{(m)}H_{(m)})^{\mathrm{T}}, \\ B_1 = f(t_l), & B_2 = 0, & B_3 = 0. \end{array}$$

In the system (16), after using the above matrices, we can solve the obtained algebraic system. So we can calculate Haar coefficients $a_{i,j}$ in (15). As a result, we can find approximate solutions of $u_j(t), j = 1, 2, 3$ in the system (3).

4. **Numerical simulation and discussion.** This section consists of three parts in order to simulate the proposed numerical method with three different types of pollution sources imposed to the Lake 1. The three cases of pollutant sources regarding to their frequency of release are classified as impulse released source, exponentially decaying released source, and periodic released source. For each case a significant numerical example is presented to show the accuracy and efficiency of the proposed method. All approximate solutions are performed with an algorithm written in a software, `Mathematica 11.3`. Also the exact solutions are obtained by using `DSolve` tool in `Mathematica 11.3` for comparison. Without loss of generality, in the all cases we choose the parameters as $V_1 = 2900\text{km}^3$, $V_2 = 850\text{km}^3$, $V_3 = 1180\text{km}^3$, $F_{12} = 24\text{km}^3/\text{year}$, $F_{13} = 22\text{km}^3/\text{year}$, $F_{21} = 14\text{km}^3/\text{year}$, $F_{23} = 18\text{km}^3/\text{year}$, $F_{31} = 32\text{km}^3/\text{year}$, $F_{32} = 8\text{km}^3/\text{year}$. Besides, the initial conditions are given by $u_1(0) = 0$, $u_2(0) = 0$, and $u_3(0) = 0$.

4.1. **Impulse imposed pollutant model.** The impulse released pollutant model describes the behavior of the pollutants that have been imposed to the Lake 1 only once. In this case functions of pollutant have a spike, then the function is zero everywhere else. The spike occurs the time at when the waste was dumped. This case can be interpreted by the function $f(t) = \omega$ where ω is a constant. This case can be sampled as dumping one barrel of chemicals into a lake at time zero. In the following example this process is illustrated by the proposed numerical method.

Example 4.1. We assume $\omega = 100$ then $f(t) = 100$. Hence, system (3) turns into

$$\begin{cases} \frac{\mathrm{d}u_1}{\mathrm{d}t} = \frac{14}{850}u_2(t) + \frac{32}{1180}u_3(t) + 100 - \frac{24}{2900}u_1(t) - \frac{22}{2900}u_1(t), \\ \frac{\mathrm{d}u_2}{\mathrm{d}t} = \frac{24}{2900}u_1(t) + \frac{8}{1180}u_3(t) - \frac{14}{850}u_2(t) - \frac{18}{850}u_2(t), \\ \frac{\mathrm{d}u_3}{\mathrm{d}t} = \frac{22}{2900}u_1(t) + \frac{18}{850}u_2(t) - \frac{32}{1180}u_3(t) - \frac{8}{1180}u_3(t). \end{cases} \tag{17}$$

Approximate numerical results for (17) are given in the Table 1 and 2. The illustration of both the exact and the approximate results are presented in Figure 2 and 3. Regarding the graphical representation, we observe the numerical solutions proposed by Haar wavelets, and the exact solutions are in good agreement. Moreover regarding to the results in each table, it is seen that the absolute error of each result decrease significantly while the interpolation level m increases.

TABLE 1. Numerical results for the case of the *impulse input imposed pollutant source* for $m = 8$.

t	**App. sol. of u_1**	**Abs. error in u_1**	**App. sol. of u_2**	**Abs. error in u_2**	**App. sol. of u_3**	**Abs. error in u_3**
0	0	0	0	0	0	0
0.2	22.9684	3.00002	0.0164893	0.0000103978	0.0151401	5.40755×10^{-6}
0.4	41.8738	2.00003	0.0657719	0.0000194067	0.0604641	0.0000101545
0.6	57.7167	1.99995	0.147536	0.0000303268	0.135809	0.0000159672
0.8	76.4975	2.99994	0.26148	0.0000389783	0.241017	0.0000206502
1	99.2168	0.0000745642	0.407297	0.0000486384	0.375927	0.0000259258

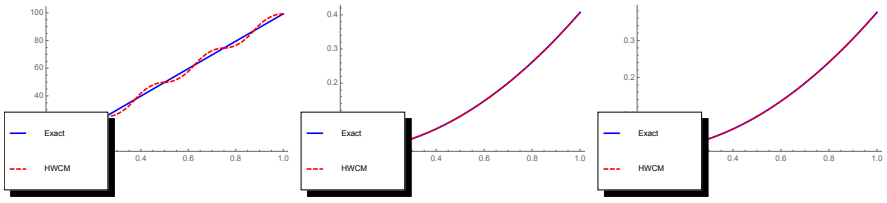

(A) (B) (C)

FIGURE 2. Graphical representation of approximate and exact solutions of Example 4.1 for $m = 8$ of (**a**) the function $u_1(t)$ (pollution in Lake 1), (**b**) the function $u_2(t)$ (pollution in Lake 2), and (**c**) the function $u_3(t)$ (pollution in Lake 3).

TABLE 2. Numerical results for the case of the *impulse input imposed pollutant source* for $m = 256$.

t	**App. sol. of u_1**	**Abs. error in u_1**	**App. sol. of u_2**	**Abs. error in u_2**	**App. sol. of u_3**	**Abs. error in u_3**
0	0	0	0	0	0	0
0.2	20.0309	0.0625	0.0164996	9.84289×10^{-9}	0.0151455	5.11793×10^{-9}
0.4	39.78	0.09375	0.0657913	1.95302×10^{-8}	0.0604743	1.02186×10^{-8}
0.6	59.8104	0.09375	0.147566	2.90455×10^{-8}	0.135825	1.52923×10^{-8}
0.8	79.4349	0.0624999	0.261519	3.83733×10^{-8}	0.241038	2.03287×10^{-8}
1	99.2167	7.28163×10^{-8}	0.407345	4.74981×10^{-8}	0.375953	2.53183×10^{-8}

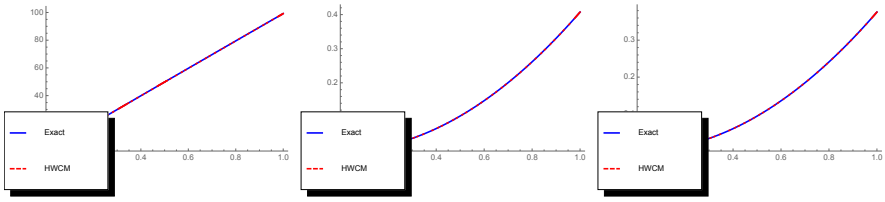

(A) (B) (C)

FIGURE 3. Graphical representation of approximate and exact solutions of Example 4.1 for $m = 256$ of (**a**) the function $u_1(t)$ (pollution in Lake 1), (**b**) the function $u_2(t)$ (pollution in Lake 2), and (**c**) the function $u_3(t)$ (pollution in Lake 3).

4.2. **Exponentially decaying imposed pollutant model.** This case is assumed when heavy dumping waste is under consideration. A factory situated near the Lake 1 stores its wastage and disposes it after a few days period. In this case function of the pollutant input would be in the form $f(t) = \delta e^{-\omega t}$. The following example illustrates the lake pollution model with exponentially decaying release of the pollutant source.

Example 4.2. In this example, we assume $\delta = 200$ and $\omega = 10$ then we have $f(t) = 200e^{-10t}$. So (3) becomes

$$\begin{cases} \frac{du_1}{dt} = \frac{14}{850}u_2(t) + \frac{32}{1180}u_3(t) + 200e^{-10t} - \frac{24}{2900}u_1(t) - \frac{22}{2900}u_1(t), \\ \frac{du_2}{dt} = \frac{24}{2900}u_1(t) + \frac{8}{1180}u_3(t) - \frac{14}{850}u_2(t) - \frac{18}{850}u_2(t), \\ \frac{du_3}{dt} = \frac{22}{2900}u_1(t) + \frac{18}{850}u_2(t) - \frac{32}{1180}u_3(t) - \frac{8}{1180}u_3(t). \end{cases} \tag{18}$$

Approximate numerical results for (18) are given in the Table 3 and 4. The illustration of both the exact and the approximate results are presented in Figure 4 and 5. Regarding Figure 4 and 5, we observe the approximate solutions proposed by Haar wavelets, and the exact solutions are in good agreement except for the function $u_1(t)$. From, Figure 4(**a**) and 5(**a**) it is seen that, we need high interpolation level to approximate the exact solution of the function $u_1(t)$. In addition to the graphical representation, it is seen from each table, the absolute error of each result decrease dramatically while the interpolation level m increases.

TABLE 3. Numerical results for the case of the pollutant source is exponential decaying for $m = 8$.

t	**App. sol. of u_1**	**Abs. error in u_1**	**App. sol. of u_2**	**Abs. error in u_2**	**App. sol. of u_3**	**Abs. error in u_3**
0	0	0	0	0	0	0
0.2	21.1544	3.89703	0.0158795	0.00284471	0.0145808	0.00261002
0.4	21.6476	2.10907	0.0445744	0.00499602	0.0409975	0.00459647
0.6	15.2365	4.55673	0.0747691	0.00702142	0.0688998	0.00647562
0.8	13.554	6.22018	0.104924	0.00900802	0.0968779	0.00832662
1	18.4945	1.2239	0.134828	0.0109746	0.124735	0.0101665

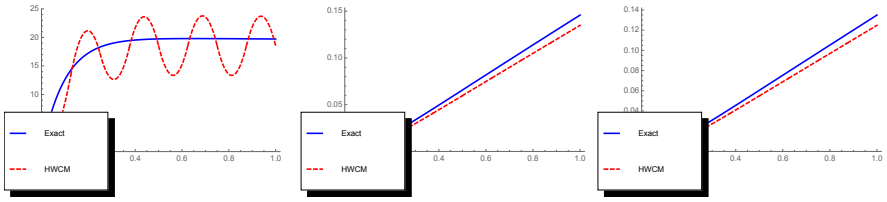

(A) (B) (C)

FIGURE 4. Graphical representation of approximate and exact solutions of Example 4.2 for $m = 8$ of (**a**) the function $u_1(t)$ (pollution in Lake 1), (**b**) the function $u_2(t)$ (pollution in Lake 2), and (**c**) the function $u_3(t)$ (pollution in Lake 3).

TABLE 4. Numerical results for the case of the pollutant source is exponential decaying for $m = 256$.

t	**App. sol. of u_1**	**Abs. error in u_1**	**App. sol. of u_2**	**Abs. error in u_2**	**App. sol. of u_3**	**Abs. error in u_3**
0	0	0	0	0	0	0
0.2	17.3813	0.123881	0.0187212	3.00622×10^{-6}	0.0171881	2.75854×10^{-6}
0.4	19.3498	0.188703	0.0495652	5.197×10^{-6}	0.0455892	4.78187×10^{-6}
0.6	19.9795	0.18621	0.0817833	7.25942×10^{-6}	0.0753687	6.69578×10^{-6}
0.8	19.6479	0.126229	0.113923	9.28787×10^{-6}	0.105196	8.58611×10^{-6}
1	19.7171	0.00124969	0.145791	0.0000112953	0.134891	0.0000104645

4.3. **Periodic imposed pollutant model.** Most of the industrial waste sources work during daytime so they produce more pollutant during a daytime more than a nighttime. Therefore in such situations pollutant could be represented by a periodic function $f(t) = p\left(1 + \omega \sin\left(\frac{2\pi}{T}t\right)\right)$ is considered as a pollutant function where p is the average input concentration of pollutant, ω s the amplitude of fluctuations and T is the period of fluctuations. Note that the peak value of pollutant function is $p(1+\omega)$. Next example illustrates the lake pollution model with periodic pollutant source.

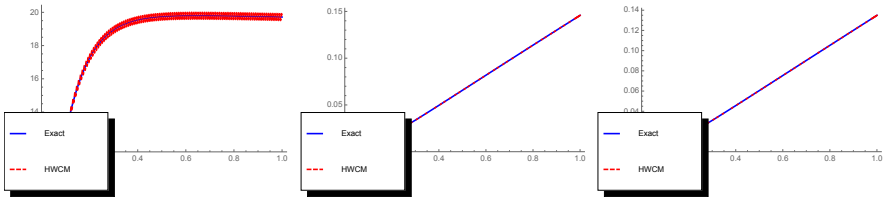

(A) (B) (C)

FIGURE 5. Graphical representation of approximate and exact solutions of Example 4.2 for $m = 256$ of (**a**) the function $u_1(t)$ (pollution in Lake 1), (**b**) the function $u_2(t)$ (pollution in Lake 2), and (**c**) the function $u_3(t)$ (pollution in Lake 3).

Example 4.3. If $p = 1$, $\omega = 1$ and $T = 2\pi$ then the pollutant function would be $f(t) = 1 + \sin(t)$. Thus, system (3) becomes

$$\begin{cases} \frac{du_1}{dt} = \frac{14}{850}u_2(t) + \frac{32}{1180}u_3(t) + 1 + \sin(t) - \frac{24}{2900}u_1(t) - \frac{22}{2900}u_1(t), \\ \frac{du_2}{dt} = \frac{24}{2900}u_1(t) + \frac{8}{1180}u_3(t) - \frac{14}{850}u_2(t) - \frac{18}{850}u_2(t), \\ \frac{du_3}{dt} = \frac{22}{2900}u_1(t) + \frac{18}{850}u_2(t) - \frac{32}{1180}u_3(t) - \frac{8}{1180}u_3(t). \end{cases} \tag{19}$$

Approximate results for (19) are given in the Table 5 and 6. The illustration of both the exact and the approximate results are presented as Figure 6 and 7. We see from the graphical representation, the numerical solutions proposed by Haar wavelets, and the exact solutions are in good agreement. Regarding to the results in each table, it is seen that the absolute errors decrease significantly while the interpolation level m increases.

TABLE 5. Numerical results for the case of the *periodic imposed pollutant source* for $m = 8$.

t	**App. sol. of u_1**	**Abs. error in u_1**	**App. sol. of u_2**	**Abs. error in u_2**	**App. sol. of u_3**	**Abs. error in u_3**
0	0	0	0	0	0	0
0.2	0.249602	0.0300057	0.000178068	2.08508×10^{-6}	0.000163497	1.96112×10^{-6}
0.4	0.497558	0.0200493	0.000748935	3.8634×10^{-6}	0.000688452	3.6487×10^{-6}
0.6	0.751366	0.0199072	0.0017721	5.90008×10^{-6}	0.001631	5.59805×10^{-6}
0.8	1.06715	0.0298126	0.00330008	7.43142×10^{-6}	0.00304105	7.08325×10^{-6}
1	1.44966	0.000281844	0.00537877	8.97633×10^{-6}	0.00496263	8.59806×10^{-6}

TABLE 6. Numerical results for the case of the *periodic imposed pollutant source* for $m = 256$.

t	**App. sol. of u_1**	**Abs. error in u_1**	**App. sol. of u_2**	**Abs. error in u_2**	**App. sol. of u_3**	**Abs. error in u_3**
0	0	0	0	0	0	0
0.2	0.220221	0.000625009	0.000175985	1.97563×10^{-9}	0.000161538	1.8579×10^{-9}
0.4	0.476572	0.000937457	0.000745076	3.87845×10^{-9}	0.000684807	3.66306×10^{-9}
0.6	0.77221	0.0009376	0.00176621	5.66633×10^{-9}	0.00162541	5.37572×10^{-9}
0.8	1.09634	0.000624822	0.00329265	7.30236×10^{-9}	0.00303397	6.96049×10^{-9}
1	1.44937	2.75122×10^{-7}	0.0053698	8.75757×10^{-9}	0.00495404	8.38886×10^{-9}

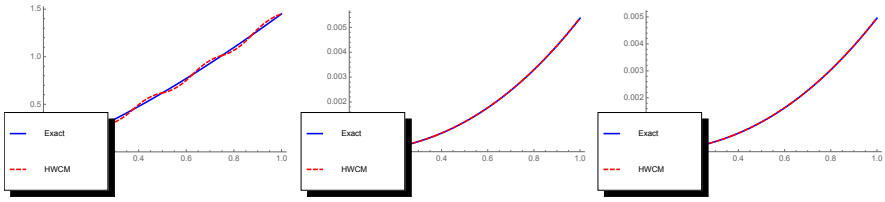

(A) (B) (C)

FIGURE 6. Graphical representation of approximate and exact solutions of Example 4.3 for $m = 8$ of (**a**) the function $u_1(t)$ (pollution in Lake 1), (**b**) the function $u_2(t)$ (pollution in Lake 2), and (**c**) the function $u_3(t)$ (pollution in Lake 3).

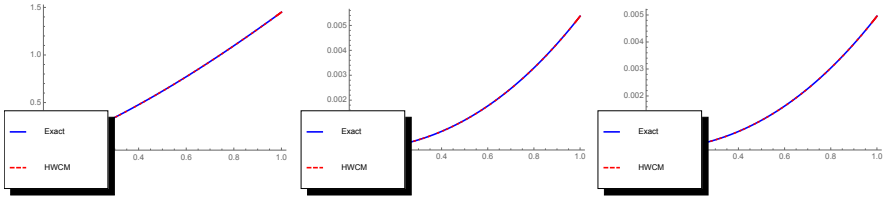

(A) (B) (C)

FIGURE 7. Graphical representation of approximate and exact solutions of Example 4.3 for $m = 256$ of (**a**) the function $u_1(t)$ (pollution in Lake 1), (**b**) the function $u_2(t)$ (pollution in Lake 2), and (**c**) the function $u_3(t)$ (pollution in Lake 3).

5. **Conclusion.** In this paper, the model of interconnected artificial three lakes with single directional flow between them is developed to monitor the contamination in the lakes. During the model developing process two well-known mathematical models in biology, the cell compartment model and the lake pollution model are used. Artificial lakes are assumed like cell compartments and the flow between them is considered as traveling molecules between the cells. The model (3) has been simulated by three different types of pollutant sources, namely impulse imposed pollutant source, exponentially decaying imposed pollutant source, and periodic imposed pollutant source. The system of differential equations implementing this model is solved with the Haar wavelet collocation method. Approximate results are compared with the exact ones. Detailed comparison between the exact results and the results obtained by Haar wavelet collocation method shows the accuracy of the proposed scheme and proves the applicability of the proposed method to the environmental pollution problem. As a result it can be said that, the Haar wavelet collocation method can be successfully used to solve pollution of the lake system model.

For future studies, this study could be extended to the real world problems by focusing on the lake systems of Great Mazurian Lakes in Poland, or Lake Tempe, Lake Buaya, and Lake Sidenreng in North Indonesia. Moreover, the model developed in this study could be extended with fractional order derivatives by including the memory effect to (3) for more realistic results. Also, some researchers may compare the results of this study with other computational methods.

Acknowledgments. The author thank the editor and anonymous referees for their valuable comments and suggestions leading to improvement of this paper.

REFERENCES

[1] J. Aguirre and D. Tully, Lake pollution model, (1999), Available from: https://mse.redwoods.edu/darnold/math55/DEProj/Sp99/DarJoel/lakepollution.pdf.

[2] I. Aziz and S. Islam, New algorithms for the numerical solution of nonlinear Fredholm and Volterra integral equations using Haar wavelets, *J. Comput. Appl. Math.*, **239** (2013), 333–345.

[3] B. Benhammouda, H. Vazquez-Leal and L. Hernandez-Martinez, A collocation approach to solving the model of pollution for a system of lakes, *Discrete Dyn. Nat. Soc.*, **2014** (2014), Art. ID 645726.

[4] İ. Çelik, Haar wavelet method for solving generalized Burgers-Huxley equation, *Arab J. Math. Sci.*, **18** (2012), 25–37.

[5] C. F. Chen and C. H. Hsiao, Haar wavelet method for solving lumped and distributed-parameter systems, *IEE Proc. Control Theory Appl.*, **144** (1997), 87–94.

[6] G. Hariharan and K. Kannan, Haar wavelet method for solving some nonlinear parabolic equations, *J. Math. Chem.*, **48** (2010), 1044–1061.

[7] G. Hariharan, K. Kannan, K. R. Sharma, Haar wavelet in estimating depth profile of soil temperature, *Appl. Math. Comput.*, **210** (2009), 119–125.

[8] G. Hariharan, K. Kannan and K. R. Sharma, Haar wavelet method for solving Fisher's equation, *Appl. Math. Comput.*, **211** (2009), 284–292.

[9] S. Islam, B. Šarler and I. Aziz and F. Haq, Haar wavelet collocation method for the numerical solution of boundary layer fluid flow problems, *Int. J. Therm. Sci.*, **50** (2011), 686–697.

[10] M. A. Khanday, A. Rafiq and K. Nazir, Mathematical models for drug diffusion through the compartments of blood and tissue medium, *Alexandria J. Med.*, **53** (2017), 245–249.

[11] Ü. Lepik, Numerical solution of differential equations using Haar wavelets, *Math. Comput. Simulation*, **68** (2005), 127–143.

[12] Ü. Lepik, Haar wavelet method for nonlinear integro-differential equations, *Appl. Math. Comput.*, **176** (2006), 324–333.

[13] Ü. Lepik, Numerical solution of evolution equations by the Haar wavelet method, *Appl. Math. Comput.*, **185** (2007), 695–704.

[14] Y. Li and W. Zhao, Haar wavelet operational matrix of fractional order integration and its applications in solving the fractional order differential equations, *Appl. Math. Comput.*, **216** (2010), 2276–2285.

[15] Ö. Oruç, F. Bulut and A. Esen, A numerical treatment based on Haar wavelets for coupled KdV equation, *Int. J. Optim. Control. Theor. Appl. IJOCTA*, **7** (2017), 195–204.

[16] M. Rehman and R. A. Khan, A numerical method for solving boundary value problems for fractional differential equations, *Appl. Math. Model.*, **36** (2012), 894–907.

[17] M. Rehman and R. A. Khan, Numerical solutions to initial and boundary value problems for linear fractional partial differential equations, *Appl. Math. Model.*, **37** (2013), 5233–5244.

[18] H. Saeedi, N. Mollahasani, M. Moghadam and G. Chuev, An operational Haar wavelet method for solving fractional Volterra integral equations, *Int. J. Appl. Math. Comput. Sci.*, **21** (2011), 535–547.

[19] I. Singh and S. Kumar, Approximate solution of convection-diffusion equations using a Haar wavelet method, *Ital. J. Pure Appl. Math.*, **35** (2015), 143–154.

[20] J. Duintjer Tebbens, M. Azar, E. Friedmann, M. Lanzendörfer and P. Pávek, Mathematical models in the description of pregnane X receptor (PXR)-regulated cytochrome P450 enzyme induction, *Int. J. Mol. Sci.*, **19** (2018), 1785.

[21] S. G. Venkatesh, S. K. Ayyaswamy and G. Hariharan, Haar wavelet method for solving initial and boundary value problems of Bratu-type, *Int. J. Comput. Math. Sci.*, **4** (2010), 286–289.

[22] Ş. Yüzbaşı, N. Şahin and M. Sezer, A collocation approach to solving the model of pollution for a system of lakes, *Math. Comput. Model.*, **55** (2012), 330–341.

Received April 2019; revised May 2019.

E-mail address: veyselfuat.hatipoglu@mu.edu.tr